Continuous methane measurements from a late Holocene Greenland ice core: Atmospheric and in-situ signals

Rachael H. Rhodes [a,*], Xavier Faïn [b], Christopher Stowasser [c], Thomas Blunier [c], Jérôme Chappellaz [b], Joseph R. McConnell [d], Daniele Romanini [e], Logan E. Mitchell [a], Edward J. Brook [a]

[a] College of Earth, Ocean and Atmospheric Sciences, Oregon State University, Corvallis OR, USA
[b] UJF-Grenoble 1/CNRS, Laboratoire de Glaciologie et Géophysique de l'Environnement (LGGE) UMR 5183, Grenoble F-38041, France
[c] Center for Ice and Climate, Niels Bohr Institute, University of Copenhagen, Copenhagen, Denmark
[d] Division of Hydrologic Sciences, Desert Research Institute, Reno NV, USA
[e] UJF-Grenoble 1/CNRS, LIPhy UMR 5588, Grenoble F-38041, France

ARTICLE INFO

ABSTRACT

Ancient air trapped inside bubbles in ice cores can now be analysed for methane concentration utilising a laser spectrometer coupled to a continuous melter system. We present a new ultra-high resolution record of atmospheric methane variability over the last 1800 yr obtained from continuous analysis of a shallow ice core from the North Greenland Eemian project (NEEM-2011-S1) during a 4-week laboratory-based measurement campaign. Our record faithfully replicates the form and amplitudes of multi-decadal oscillations previously observed in other ice cores and demonstrates the detailed depth resolution (5.3 cm), rapid acquisition time (30 m day^{-1}) and good long-term reproducibility (2.6%, 2σ) of the continuous measurement technique.

In addition, we report the detection of high frequency ice core methane signals of non-atmospheric origin. Firstly, measurements of air from the firn–ice transition region and an interval of ice core dating from 1546–1560 AD (gas age) resolve apparently quasi-annual scale methane oscillations. Traditional gas chromatography measurements on discrete ice samples confirm these signals and indicate peak-to-peak amplitudes of ca. 22 parts per billion (ppb). We hypothesise that these oscillations result from staggered bubble close-off between seasonal layers of contrasting density during time periods of sustained multi-year atmospheric methane change. Secondly, we report the detection of abrupt (20–100 cm depth interval), high amplitude (35–80 ppb excess) methane spikes in the NEEM ice that are reproduced by discrete measurements. We show for the first time that methane spikes present in thin and infrequent layers in polar, glacial ice are accompanied by elevated concentrations of carbon- and nitrogen-based chemical impurities, and suggest that biological in-situ production may be responsible.

1. Introduction

Records of past atmospheric methane concentration derived from ancient air trapped in ice cores help to define our understanding of the global carbon cycle and its interaction with climate on many timescales (e.g., Blunier and Brook, 2001; Loulergue et al., 2008; Mitchell et al., 2011). Specifically, records of past methane variability are extremely valuable for understanding the relative strength and spatial distribution of methane sources and sinks (Brook et al., 2000) and their response to climate change (Lelieveld et al., 1998; Menviel et al., 2011; Singarayer et al., 2011). Furthermore, methane has become an important tool for global synchronization of ice core records as a result of its large and frequent variations on time scales of interest for paleoclimate reconstruction (Blunier et al., 2007).

Ice core methane mixing ratios are typically determined by gas chromatography on discrete pieces of ice using a wet (e.g., Flückiger et al., 2002; Grachev et al., 2007, 2009) or dry (e.g., Blunier et al., 1995; Etheridge et al., 1998; MacFarling Meure et al., 2006) extraction method. Discrete analysis using these methods can be both highly accurate and reproducible (Mitchell et al., 2011) but it is relatively labour- and time-intensive, and, depending on sample spacing, some true signal variability will be aliased. Recently, a powerful technique for efficient, high resolution, continuous measurement of ice core methane using laser spectroscopy has been

developed (Stowasser et al., 2012). During two consecutive seasons at the North Greenland Eemian (NEEM) ice core project drill site, a system of gas extraction was coupled to the continuous flow analysis (CFA) setup used for chemical analysis of the NEEM ice (Bigler et al., 2011; Kaufmann et al., 2008). Gas released from bubbles in the ice, previously considered as a waste product, was extracted and analysed in real time at a precision equalling or surpassing discrete measurements (Stowasser et al., 2012). Many of the techniques and solutions devised at NEEM were employed for our analytical campaign at the Desert Research Institute (DRI), Reno, NV, USA, in which methane concentrations were measured continuously on the 410 m NEEM-2011-S1 (hereafter referred to as NEEMS1) ice core to reconstruct methane concentrations of the past 1800 yr.

Stowasser et al. (2012) reported a depth resolution (the minimal depth range for which a damped version of a periodic input signal can be detected) of 5 cm for continuous methane measurements along the main NEEM core. This is significantly better than that of the highest resolution routine discrete measurement programs, which are typically conducted at metre-scale resolution (e.g., Mitchell et al., 2011). Significantly, the excellent depth resolution of the continuous technique equates to a temporal resolution that allows detection of all "climatically relevant" variations in methane down to 1980 m depth in the NEEM core (Stowasser et al., 2012). Effectively, this means that any oscillation in atmospheric methane will be resolvable in the ice core record, providing that it survives the processes of signal smoothing, which occur in the firn pack during densification, prior to complete bubble close-off (Spahni et al., 2003). The degree of smoothing in the firn varies between ice cores, and is primarily dependent on temperature and accumulation rate (Schwander et al., 1997). For Holocene ice at NEEM the gas age distribution (width at half maximum) at the base of firn is ca. 32 yr (Buizert et al., 2012) and therefore any higher frequency variability in the atmosphere, for example, the seasonal cycle in methane concentration, cannot be preserved in the ice core gas record.

In this study we demonstrate that our efficient and precise continuous measurements on the NEEMS1 ice core produce an ultra-high resolution atmospheric history of methane for the last 1800 yr, which replicates multi-decadal variability previously observed. Further key findings of this paper concern high frequency methane signals that cannot be of atmospheric origin. Reproducible annual scale methane oscillations that may be artifacts of heterogeneous bubble close-off in the firn are detected. We also report the presence of abrupt, high amplitude methane spikes in the ice that likely result from biological in-situ production of methane.

2. Method

2.1. NEEM-2011-S1 ice core drilling

The NEEMS1 ice core was drilled in northern Greenland to 410 m depth in 2011. The borehole location was 200 m from the main NEEM borehole (77.45°N, 51.06°W). Drill fluid was used to maintain the diameter of the borehole below 80 m depth. The ice core was cut in the field, and later also at DRI, to produce two equi-dimensional ($55 \times 3.4 \times 3.4$ cm) sticks, designated M cut and B cut, for continuous analysis.

2.2. Analytical system

The continuous melter system at DRI (McConnell and Edwards, 2008; McConnell et al., 2007, 2002) was modified to include two sealed debubblers, a gas extraction box (detailed description in Stowasser et al., 2012) and a laser spectrometer (Fig. 1, letters in parentheses in following text are displayed on figure). A mixture of melted ice and gas bubbles, extracted from the middle concentric ring of the melterhead (A) (2.73 cm^2 area), was pumped to the first sealed debubbler (B) (internal volume 1.8 cm^3). All the gas bubbles and approximately 30% of the water were pushed on towards a second debubbler (C) (internal volume
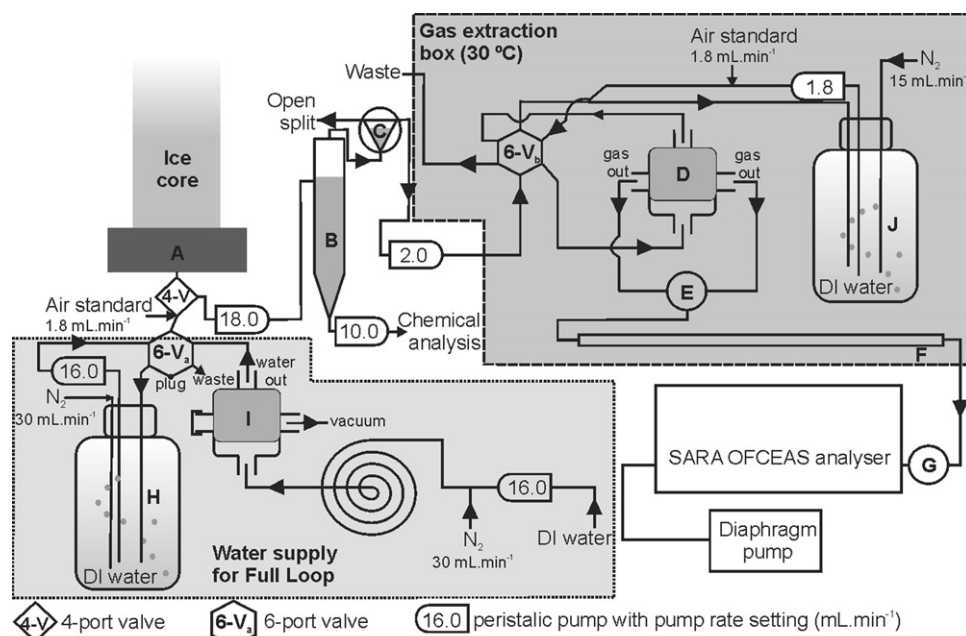
Fig. 1. Schematic of the continuous ice core gas analytical setup. Ice core melting occurs at a heated melterhead (A), sample is pumped to a debubbler (B), open split (C) and into the gas extraction box. The gas extraction system consists of a gas-permeable membrane module (Liqui-Cel, G591) (D) and a homemade Nafion dryer (2 m length, 0.3 mm inner diameter) (F). Gas flow is monitored by a pressure transducer (Omega Inc.) (E) and controlled by a back-pressure controller (IQ$^+$ Flow, Bronkhorst Inc.) (G). Degassed water from either a N$_2$-flushed 2 L bottle (H) or a gas-permeable membrane module (I) (position of 6-V_a determines this) is mixed with synthetic air standard (position of 6-V_a determines which) and introduced to the system via a 4-port valve below the melterhead. when no ice core is being melted.

0.7 cm^3) that functioned as an open split to prevent pressure buildup in the system (Schüpbach et al., 2009). The water and gas bubble mixture (50:50) was actively pumped from this debubbler to the gas extraction box.

Inside the temperature-controlled (30 ± 0.1 °C) gas extraction box, gas was extracted from the water stream inside a polycarbonate module containing a densely-packed gas-permeable membrane (D) (internal volume 5.4 cm^3). Gas sample was pulled from both "gas arms" of the module to minimise dead volume. The pressure gradient across the gas permeable membrane module was generated by a diaphragm pump downstream of the laser spectrometer and controlled by a back-pressure controller (G) (Fig. 1). The gas pressure recorded downstream of the module (E) was typically 780–830 mbar for ice core sample and was sufficiently low to extract all visible air bubbles from the sample mixture. A Nafion (PermaPure) dryer (F) with a 25 mL min^{-1} purge flow of ultra-pure N$_2$ (Airgas > 99.9995% purity) dried the humid sample gas to < 0.01% H$_2$O content before entry into the laser spectrometer.

The laser spectrometer SARA (Spectroscopy by Amplified Resonant Absorption, developed at Laboratoire Interdisciplinaire de Physique, Grenoble, France) utilises a technique called Optical Feedback Cavity Enhanced Absorption Spectroscopy (OFCEAS) (Morville et al., 2005; Romanini et al., 2006) and yields measurements of carbon monoxide (CO), methane (CH$_4$), and water (H$_2$O) by fitting absorption spectra in the 2325.1–2325.5 nm wavelength range. The analyser is specifically adapted for ice core analysis where only a limited volume of gas is available. A PID-controlled outlet valve maintains a pressure of 20 mbar in the 12 cm^3 cavity of the instrument, resulting in only 0.24 cm^3 STP of gas in the cavity, and a renewal time of 10 s for a typical gas flow rate of 1.5 mL min^{-1}. CO measurements from this campaign will be reported separately (Faïn et al., in preparation).

2.3. Calibration

Three synthetic air standards (Table 1) were measured directly by the laser spectrometer to produce a linear calibration curve with a correlation coefficient R^2 > 99.999% (Fig. S1A). In order to place methane measurements produced by the laser spectrometer onto the NOAA2004 scale (Dlugokencky et al., 2005), the linear relationship derived from only the two air standards that have been very precisely calibrated (Table 1) was used (Fig. S1B).

Continuous laser-based analysis conducted in the field at NEEM produced significantly lower methane mixing ratios than traditional discrete analysis. Methane has a higher solubility than air, which causes a portion of the methane released from the gas bubbles to dissolve in the melted ice core sample (Stowasser et al., 2012). In order to improve our understanding of this offset, we attempted to replicate the conditions experienced by the ice core water-gas mixture between the melterhead and the laser spectrometer. As melting ice contains 10% air, a 10:90 mixture of synthetic air and degassed water was introduced into the system via a 4-port valve directly after the melterhead (Fig. 1). The water was sourced from either (1) a 2 L reservoir degassed by constantly bubbling ultra-pure N$_2$ through it (Fig. 1H) or (2) an in-house deionized (DI) water supply degassed continuously by mixing it with ultra-pure N$_2$ and passing it through another gas permeable membrane module with a vacuum applied (Fig. 1G). As the degree of degassing achieved by the second method was not consistent, only results produced using degassed water from the 2 L reservoir were used for the solubility correction (see Section 2.5.2). The air–water mixture followed the same path through the system as the ice core sample before being analysed by the laser spectrometer. This pathway for synthetic standard analysis was designated the "full loop".

2.4. System operation

Ice core was melted at a mean rate of 6 cm min^{-1} and 8 m of ice core were melted continuously by loading successive lengths of core on top of the already melting section. M cut ice sticks were melted successively from bottom to top of the core. Selected B cut sticks were analysed as replicates. The timing of the start and end of each core length, and of any additional breaks in the core that passed over the melterhead, were recorded. After each 8 m melting run ended, the 4-port valve underneath the melterhead was switched to provide a synthetic air–water mixture via the full loop (Section 2.3).

To isolate the continuous gas setup from the remainder of the DRI melter system a 6-port valve (Fig. 1, 6-V_b) was switched to provide the gas extraction system with a 50:50 synthetic air standard/water mixture. This pathway was designated the "internal loop" because the gas/water mixture was generated inside the gas extraction box from a 1 L degassed water reservoir (Fig. 1J).

2.5. Data processing

2.5.1. Stability and precision

Allan variance test (Allan, 1966) results indicate that a precision (1σ) of 0.1 ppb is achieved at the optimal integration time of 11 min when dry synthetic air standard is measured directly (Supplementary Material, Fig. S2). The optimal integration time for measurements made via the full loop is ca. 5 min, which results in a precision of 0.24 ppb. As will be shown in Section 2.5.4, integrating over this time would result in significant smoothing of potentially interesting signals in the dataset so a trade-off between

Table 1

Methane concentration (ppb, reported on NOAA2004 scale) of synthetic air standards (prepared by Scott–Marrin Speciality Gases) compared to mean values of measurements conducted on dry gas directly introduced to the laser spectrometer, introduced via the internal loop, and via the full loop. Each value is the mean of several repeated measurements (number of measurements (n) displayed) conducted throughout the analytical campaign, where each of these individual measurements is a mean value of a 10 min measurement interval. The long-term precision of the continuous analytical technique is stated as 2*standard deviation (2σ) on these measurements. The 2*relative standard deviation (2RSD) is given in parentheses.

	Standard 1	Standard 2	Standard 3
Certified	384.89 ± 0.60 (0.16%)[a] $n=3$	667.30 ± 0.60 (0.09%)[a] $n=3$	1334.14 ± 11.40 (0.85%)[b] $n=11$
Direct	385.0 ± 0.42 (0.11%) $n=2$	667.5 ± 0.42 (0.06%) $n=3$	1350.7 $n=1$
Internal loop	380.5 ± 4.69 (1.23%) $n=9$	659.1 ± 3.12 (0.47%) $n=3$	–
Full loop	368.0 ± 9.49 (2.58%) $n=22$	620.3 ± 17.19 (2.77%) $n=4$	1244.1 $n=1$

[a] Calibrated by the NOAA GMD Carbon Cycle Group and reported on the NOAA2004 scale (Dlugokencky et al., 2005).
[b] Calibrated at Oregon State University (OSU) relative to a working standard on the NOAA2004 scale.

precision and depth-resolution must be made. Data presented here are integrated to 5 s and have a precision of 0.45 ppb (1σ).

2.5.2. Correction for solubility

The methane concentrations of synthetic air standards recorded in the full loop calibration mode were significantly lower than both those measured directly and via the internal loop (Table 1). Water and gas bubbles are in contact with each other through a ca. 3 m length of tubing during transport between the melterhead and the gas extraction box, corresponding to 2–3 min at the given flow rate. This allows opportunity for preferential dissolution of methane, principally relative to nitrogen (Henry's Law constants at 298.15°K: $CH_4 = 0.0014$ mol/kg bar and $N_2 = 0.0006$ mol/kg bar, (NIST, 2011)). The degree of methane dissolution remained relatively constant throughout the 4-week analytical campaign–the long-term precision (2*relative standard deviation (RSD)) is 2.6%, equivalent to 9.5 ppb, for 22 full loop measurements of 10 min length on Standard 1 (Table 1). Data from replicate ice core sticks (B cut) also exhibit good reproducibility–the mean offset between CH_4 concentrations measured in the ice core and in each of the six replicate cuts varied between 0.4% and 2.1% (Table S1).

A weighted least-squares linear regression of three different synthetic air standards measured in full loop mode on the same day of analysis against certified concentrations (Fig. S1B) produces a slope of 0.9266 ± 0.010 (2σ uncertainty, $R^2 > 0.999$), indicating that ca. 7.3% of the methane is not recovered during gas extraction. We therefore apply a correction factor of 1.079 to the entire dataset to correct for the effect of methane dissolution. We note the possibility that using N_2 to degas DI water may lead to saturation of the water with N_2 and therefore a stronger-dissolution of CH_4 relative to N_2 in the sample lines once the synthetic air standard is mixed in, leading to a slight overestimation of the solubility correction factor. Results from a recent measurement campaign, in which both N_2 and He were tested as purge gases, suggest this overestimation amounts to $<2\%$.

The accuracy of the corrected CH_4 concentrations, calculated via propagation of the error on the linear regression equation (Fig. S1B), is ± 6.2 ppb (1 standard deviation (σ)) for typical Late Holocene CH_4 concentrations (780 ppb), and ± 9.4 ppb (1σ) for CH_4 concentrations in the anthropogenic era (1400 ppb).

2.5.3. Correction for water in cavity

Evaporation of small amounts of liquid water that entered the gas lines on several occasions during the analytical campaign caused dilution of the sample gas and reduction of the measured methane concentration. Sections of the record from 125–130 m and 341–364.2 m have been corrected for this effect (details provided in Supplementary Material). Data from 364.2–374.4 m, 257.5–271.3 m, 130–137 m and 93–97 m are not presented here because they could not be corrected because the water vapour level was variable or no replicate data were available.

2.5.4. Translation to depth and sample resolution

Data series were translated from the experiment time domain to depth domain using the start/stop times recorded during melting, assuming a constant melt rate for each 55 cm core section. The time delay between the onset or cessation of ice core melting and the response of the methane signal measured by the laser spectrometer was estimated daily (2.6–4.3 min range). The uncertainty on these estimates equates to a depth uncertainty of ± 6 cm (2σ) (equivalent to 0.3 yr in age).

The extent of signal smoothing resulting from memory effects and sample dispersion was calculated by performing a step test (Supplementary Material, Fig. S3)—a switch between two synthetic air standards of different concentrations, following the methods of Stowasser et al. (2012) and Gkinis et al. (2011). 7 min of data,

equivalent to 42 cm depth, were removed from the start of each 8 m melting run to eliminate effects of sample mixing with synthetic air standard in the system. The transfer function produced by the step test defines the maximum temporal resolution of the system. At a 6 cm min^{-1} melt rate a periodic signal in the ice with a wavelength of 5.34 cm depth (Supplementary Material, Fig. S3B) can be detected, although it will be significantly dampened.

2.5.5. Data screening

The methane data were screened for contamination resulting from entry of ambient air (ca. 1900 ppb) at the melterhead during core breaks. The ambient CO concentration measured was 150 ppb, which is equal to or lower than levels in the ice core and synthetic air standards. The freezer room housing the melterhead was free of potential CO sources, such as ethanol, and air inside was circulated continuously. Thus, ambient air contamination was characterised by a sharp increase in methane concentration followed by an exponential decrease and the absence of a coincident abrupt increase in CO concentration (Supplementary Material, Fig. S4).

2.5.6. Chronology

The ice age-depth scale for the NEEM-2011-S1 ice core was developed by annual layer counting of several chemical species and is constrained by major volcanic events to an accuracy of ± 1 yr (Sigl et al., in press). This ice age scale and the calculated modern-day gas age-ice age difference (Δage) for NEEM ($182 + 3/ - 9$ yr, Buizert et al., 2012) were used to generate the gas age scale.

2.6. Discrete methane measurements

Methane concentrations were determined on 60 discrete samples to verify signals observed by continuous analysis. Samples were cut at 3 cm depth resolution and each had a mass of ~ 40 g. Air was extracted using a melt-refreeze method and methane concentrations were determined by gas chromatography (Grachev et al., 2007, 2009; Mitchell et al., 2011). Corrections for known solubility effects and blank values were made following Mitchell et al. (2011). All data are reported on the NOAA2004 scale (Dlugokencky et al., 2005).

2.7. Chemistry

During the analytical campaign, melted ice core sample was analysed continuously by inductively coupled plasma mass spectrometry (ICP-MS) and CFA for chemical species considered in this study. These analytical methods have been reported previously (McConnell and Edwards, 2008; McConnell et al., 2007, 2002).

3. Results and discussion

3.1. Methane concentrations of the past 1800 yr

We present our methane record from the NEEM-2011-S1 ice core in Fig. 2 (data available online at http://www.ncdc.noaa.gov/). We make two primary observations. Firstly, several anomalous spikes in methane are clearly visible (grey data points) and will be considered in detail in Section 3.2. Secondly, the methane concentrations of the underlying atmospheric, multi-decadal portion of the NEEMS1 record (blue) lie within the 2σ uncertainty range of the Greenland Ice Sheet Project 2 (GISP2) discrete measurements (Mitchell et al., in preparation) without any further adjustment (Fig. 2). This suggests that the full loop calibration mode successfully replicated the conditions (i.e., temperature, pressure, time) that control methane dissolution in the sample lines between the melterhead and the gas extraction module (Section 2.5.2).
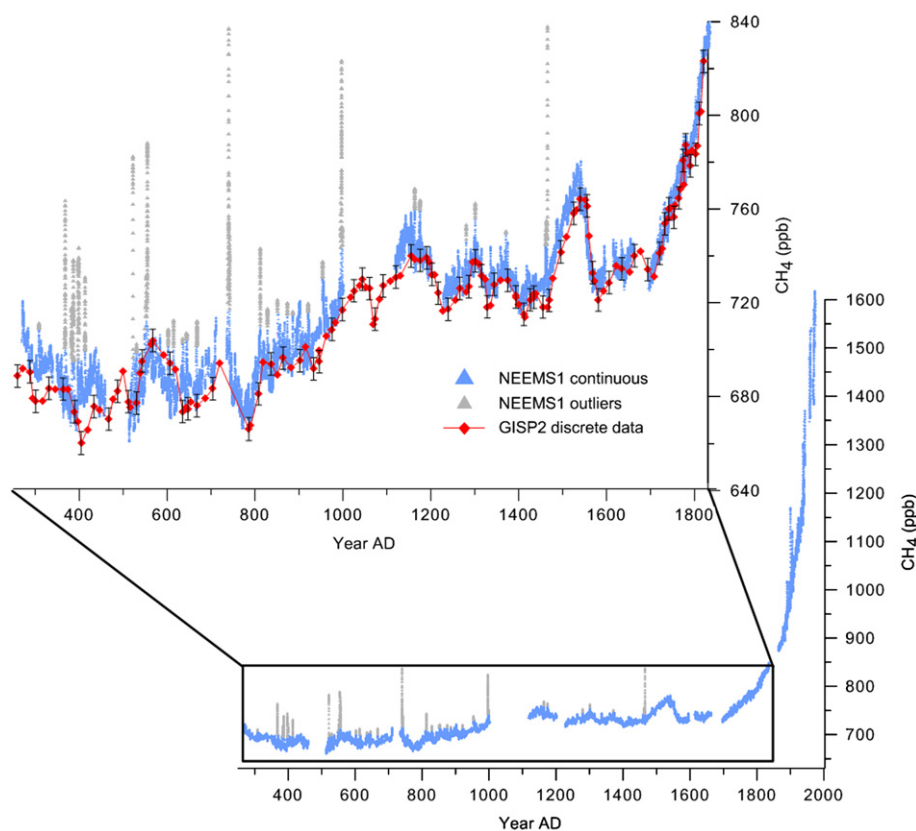
Fig. 2. NEEMS1 continuous methane record of the past 1800 yr. Outliers are 2*MAD > 15 yr running median. Methane concentrations from the GISP2 ice core (Mitchell et al., in preparation) are plotted for comparison on inset. Uncertainty bars displayed on alternate GISP2 data points are long-term reproducibility (4.8 ppb, 2σ). The GISP2 gas age scale employs a modern-day Δage of 190.1 yr, calculated using a firn transport model (Buizert et al., 2012) with firn air data for Summit, Greenland, and an ice age scale tied to the GICC05 timescale. All data are plotted on the NOAA04 calibration scale (Dlugokencky et al., 2005). (For interpretation of the references to colour in this figure, the reader is referred to the web version of this article.)

Comparison of our NEEMS1 record with the GISP2 ice core data highlights the efficiency of the continuous laser-based analytical technique for multi-decadal analysis of methane in ice cores. The multi-decadal scale variability in GISP2 methane, also observed in discrete measurements from West Antarctic Ice Sheet (WAIS) Divide (Mitchell et al., 2011) and Law Dome (Etheridge et al., 1998; MacFarling Meure et al., 2006) ice cores, is faithfully replicated in the long-term trend of our continuous measurements (Fig. 2, blue). In particular, the timing, amplitude and asymmetric form of the methane peak with a 770 ppb maximum at ca. 1550 AD are remarkably similar (Fig. 2). This demonstrates that the continuous measurement system does not smooth or distort the multi-decadal signal.

The principal shortcoming of the continuous measurement technique is the uncertainty on the absolute concentration ($\pm$6.2 ppb 1σ uncertainty on 780 ppb, Section 2.5.2). This needs to improve before data can be used for very precise work, for example, calculation of the magnitude of the methane inter-polar gradient, which typically ranges between 20 and 50 ppb (e.g., Baumgartner et al., 2012; Brook et al., 2000). Nonetheless, the fine detail, rapid acquisition time, and co-registration of the trace gas results with chemistry measurements are clearly advantages of the continuous technique.

3.2. Abrupt, high amplitude methane spikes: evidence for in-situ production

3.2.1. Identification and verification

The abrupt, high amplitude spikes in methane concentration exceeding a cut-off value of 2*MAD (median absolute deviation) >

running median are considered outliers (Fig. 2, grey points). MAD values were calculated separately for the 250–1000 AD and the 1100–1835 AD sections of the record to account for the ca. 30 ppb difference between the medians of these two sections. A running median with a window length of 15 yr is used but any window length between 5 and 40 yr produces very similar outlier identification. An atmospheric signal of a shorter period is very unlikely to survive the smoothing processes in the firn at NEEM (Spahni et al., 2003).

The possibility that ambient air contamination is responsible for the methane spikes is ruled out because the spikes are matched by increases in carbon monoxide (Fig. 3) (cf. Section 2.5.5). A second possible explanation for these methane spikes is that they are artifacts of the continuous gas analysis method, possibly resulting from extraordinary pressure or flow conditions. To determine the likelihood of this being the case, replicate ice (B cut) from exactly equivalent depths to the anomalous methane signal at 384.8–385.6 m was analysed for methane concentration by the traditional discrete methodology (Section 2.6). The results confirm the presence of the methane spikes in the ice (Fig. 3) and negate any possibility that they are artifacts of the continuous gas analysis. Additionally, the exceptionally high resolution (3 cm spacing) discrete measurements highlight the smoothing effect of the continuous system (Section 2.5.4) at this small scale. For example, the continuous method recorded a methane spike of 67 ppb while the discrete measurements resolve a 107 ppb spike.

We identify ten major abrupt, high amplitude methane spikes that occur over 20–100 cm depth intervals in the ice core, equivalent to 2–5 yr in the time domain, and exhibit [dampened]
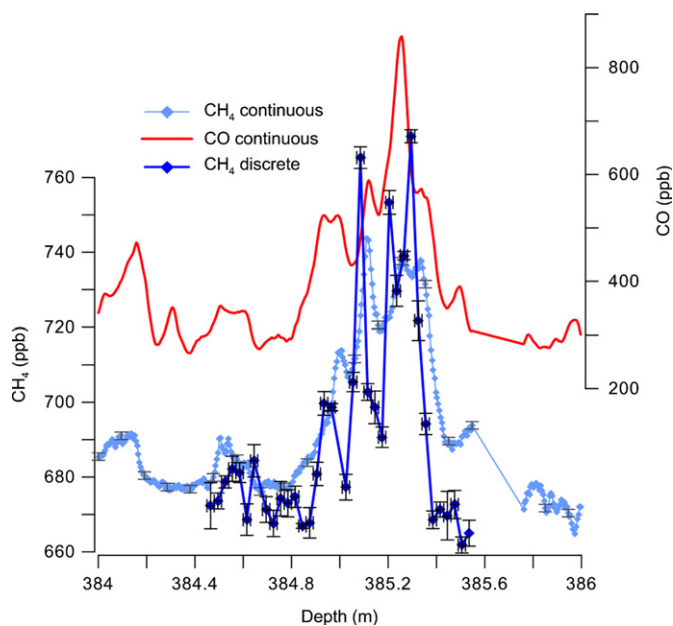
Fig. 3. Continuous CH_4 and CO concentration data and results of discrete CH_4 analyses across an abrupt, high amplitude CH_4 spike centred at 385.2 m. Y-axis uncertainty bars are 2σ. X-axis uncertainty bars indicate that a 3 cm depth interval was sampled for each discrete sample. There is a systematic depth offset between the continuous and discrete measurements varying in magnitude between 2 and 4 cm between 384.9 and 385.5 m. These offsets are within the stated depth uncertainty of ± 6 cm (2σ) on the continuous dataset and suggest an underestimation of the sample travel time between the melterhead and the analyser for this section of ice core.

maximum concentrations of 731–838 ppb, or 35–80 ppb in excess of the 2*MAD > running median cut-off (Table 2). A second one of these methane spikes was reproduced by continuous analysis of the replicate (B cut) (Fig. 4, #6). We note that the two continuous datasets have not been aligned on either axes and therefore exhibit some differences due to uncertainty on the depth estimate and the methane solubility correction (Section 2.5.2). The horizontal extent of regions with elevated methane levels within the ice cannot be quantified. However, anomalous methane (and CO) signals were recorded in adjacent ice core sticks (M and B cut) from equivalent depths that together represent a horizontal distance of 6.8 cm (Figs. 3 and 4 #6).

Any possibility that these signals are of atmospheric origin is precluded by their abrupt nature and short duration (i.e., 60 ppb increase in 2 yr) for two reasons: (1) such a high frequency signal could not survive the firn smoothing process (Spahni et al., 2003) and (2) there is no known mechanism to cause atmospheric methane levels to decrease exponentially within such a short space of time (Brook et al., 2000).

Recent measurements suggest that anomalously high methane values may be associated with melt layers (NEEM community members, 2013). During the processing of NEEMS1, each ice core stick was closely inspected for evidence of melting and no observations were recorded for the depths at which the abrupt, high amplitude methane spikes are present. Additionally, the gas flow rates recorded by the laser spectrometer and the total air content values measured on discrete samples show no anomalies. We therefore dismiss this possible explanation. The core was also inspected for fractures in which organic-rich drill fluid (Estisol 240 and Coasol) residue might have been present and affected sections were removed prior to melting. Furthermore, a test involving analysis of air inside the head-space of a drill fluid container (presumably saturated with vapour) recorded excess methane concentrations ranging between only 20 and 50 ppb. For this reason, and additionally because the physical quality of

the core improved with depth, decreasing the likelihood of drill fluid residue, and because the methane spikes are present in adjacent ice core sticks, we are confident that drill fluid contamination cannot account for the methane spikes.

3.2.2. Comparison to high resolution chemistry

In order to further characterise the rapid, high amplitude spikes in the NEEMS1 methane record, we consider high resolution chemistry measurements (Fig. 4, three examples shown). For nine of the ten largest methane spikes identified (Table 2), black carbon levels are enriched by a factor > 7, relative to the median of the entire record, with spike #5 showing an enrichment of 87-fold. Ammonium (NH_4^+) concentrations are also consistently elevated above the median for methane spikes #1–9 with relative enrichment ranging from 11 to 68-fold (Table 2). Another nitrogen-based compound, nitrate (NO_3^-), is enriched relative to the median in 7 out of 9 cases, but to lesser degree. All three of these chemical species show consistently close correspondence in depth to the methane spikes (Fig. 4). Non-sea salt sulphur (nssS), usually present in ice as sulphate (SO_4^{2-}), is enriched relative to the median at only half of the ten highest methane spikes. Redox-sensitive manganese (Mn) exhibits variable behaviour across the different methane spikes; some methane spikes have a clear enrichment in Mn associated with them (Fig. 4, #5 and #6) but others show little signal (Fig. 4, #3). A proxy for carbonate dust in Greenlandic ice, non-sea salt calcium (nssCa), shows no systematic enrichment across methane spikes, except at spike #5 (Table 2, Fig. 4). Elements such as cerium (Ce), that are abundant in alumino-silicate minerals, show similar variability to nssCa.

In summary, the abrupt, high amplitude methane spikes are closely associated with black carbon and nitrogen-based compounds present in the ice but show little relationship to inorganic chemical species derived from mineral dust. This suggests that the excess methane is the product of organic in-situ production within the ice concentrated within ice layers enriched with biomass burning end products.

3.2.3. In-situ production

It has been suggested that microorganisms can inhabit liquid veins which exist at triple grain junctions within the glacial ice matrix (Price, 2000). According to this theory, sulphuric acid and nitric acid, which are known to be concentrated in the veins (Barnes and Wolff, 2004), are utilised as energy sources in the decomposition of simple organic carbon compounds. The ice chemistry associated with in-situ methane spikes in NEEMS1 is broadly consistent with this idea—in-situ methane is associated with relatively high levels of black carbon and HNO_3^-, but not always with SO_4^{2-}. Furthermore, both inorganic and organic in-situ production of CO_2 is thought to occur in Greenlandic ice (Anklin et al., 1997; Barnola et al., 1995; Tschumi and Stauffer, 2000), thus providing an additional potential source of carbon for microorganisms. A second proposed habitat for microorganisms in glacial ice is the thin film of liquid water that surrounds dust grains, particularly clays (Price, 2007; Tung et al., 2005). Our results show little correspondence between the methane spikes and any mineral dust proxy.

One important question is whether microorganisms capable of methane production are present throughout the glacial ice column and only produce detectable levels of methane when sufficient organic compounds or nutrients are present, or whether the microorganisms are only located within the organic-rich layers. In other words, were microbes continuously deposited at the glacier surface or did they arrive with the organic material? Black carbon and NH_4^+ deposited on the Greenland Ice Sheet originate from biomass burning

Table 2

Magnitudes, depths and associated chemistry of ten most pronounced abrupt, high amplitude methane spikes. Excess CH_4 is the difference between maximum CH_4 concentration and 2*MAD+running median. Concentrations of NH_4^+, black carbon, HNO_3, nssCa, Mn and nssS are difference between the maximum concentration within the stated depth range and the median of the entire record.

#	Depth range (m)	Notes	CH_4 max. (ppb)	Excess CH_4 (ppb)	CO spike? (Y/N)	NH_4^+ (μM)	Black carbon (ng g^{-1})	HNO_3^- (μM)	nssCa (ng g^{-1})	Mn (ng g^{-1})	nssS (ng g^{-1})
1	390.5–390.9		767	66	Y	11.0	75.0	2.0	18.0	0.70	0
2	387.2–388.2	DP	739	46	Y	8.7	33.0	1.0	0	0	0
3[a]	384.6–385.5	RD	747	50	Y	5.3	32.0	2.0	0	0	0
4	382.0–382.4		731	35	Y	3.2	30.0	2.0	11.0	0.10	23.0
5[a]	362.8–363.0	RC	785	80	Y	16.0	200.0	7.2	32.0	1.90	43.0
6[a]	356.1–356.9		789	74	Y	14.0	80.0	3.4	8.0	0.20	12.0
7	321.5–322.1	DP	838	78	Y	7.0	17.0	2.3	6.0	0.30	6.3
8	307.8–308.1		742	38	Y	13.0	26.0	2.3	3.2	0.30	13.0
9	272.1–272.4		826	78	Y	2.6	2.0	1.0	5.8	0.25	33.0
10	178.1–178.4		838	77	Y	0	2.2	0	3.0	0.03	0

DP=dual peak; RD=replicated by discrete measurements; RC=replicated by continuous measurements.

[a] Plotted in Fig. 4.
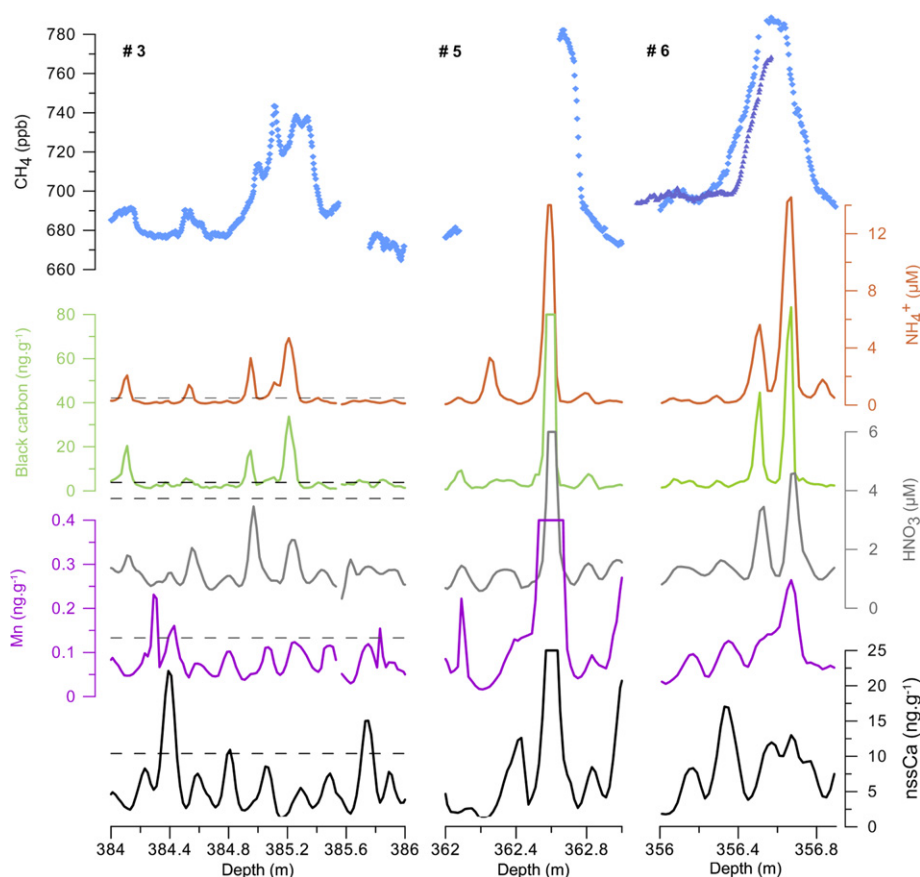
Fig. 4. Three abrupt, high amplitude methane spikes from the NEEMS1 continuous record compared to several chemical species on a depth scale. Dashed black lines are median+2*MAD concentrations of each chemical species. Methane spike #6 was replicated by continuous measurements on a replicate core (B cut) (purple–blue symbols). (For interpretation of the references to colour in this figure legend, the reader is referred to the web version of this article.)

events (McConnell et al., 2007)—not an environment where cold-tolerant microorganisms would necessarily be expected. Christner et al. (2000) isolated bacteria from several ice cores in both hemispheres and found no increase in cell count with depth, suggesting that bacteria arrive periodically with other organic or inorganic material. Rohde et al. (2008) also found evidence for episodic input of microorganisms, which they suggest is controlled by storm strength and frequency. Our record shows significantly more abrupt, high amplitude methane spikes in the record prior to 1000 AD (272 m depth) than after that time (Fig. 2). This could indicate that: (1) the microorganisms enclosed in older ice have had more time to produce methane, and/or (2) stormier conditions prior to 1000 AD transported higher quantities of microorganisms, carbon and nutrients to the NEEM site. We would argue against the second possibility because the chemistry record from NEEMS1 offers no evidence for increased storminess.

Previous exploration of in-situ methane production in polar ice has focused on accreted ice or basal ice that is both physically disturbed and rich in impurities. Anomalously high methane mixing ratios (> 4000 ppmv) measured in the deepest GISP2 ice core have been linked to relatively high microbial levels, detected using an auto-fluorescence technique (Tung et al., 2005). Combined
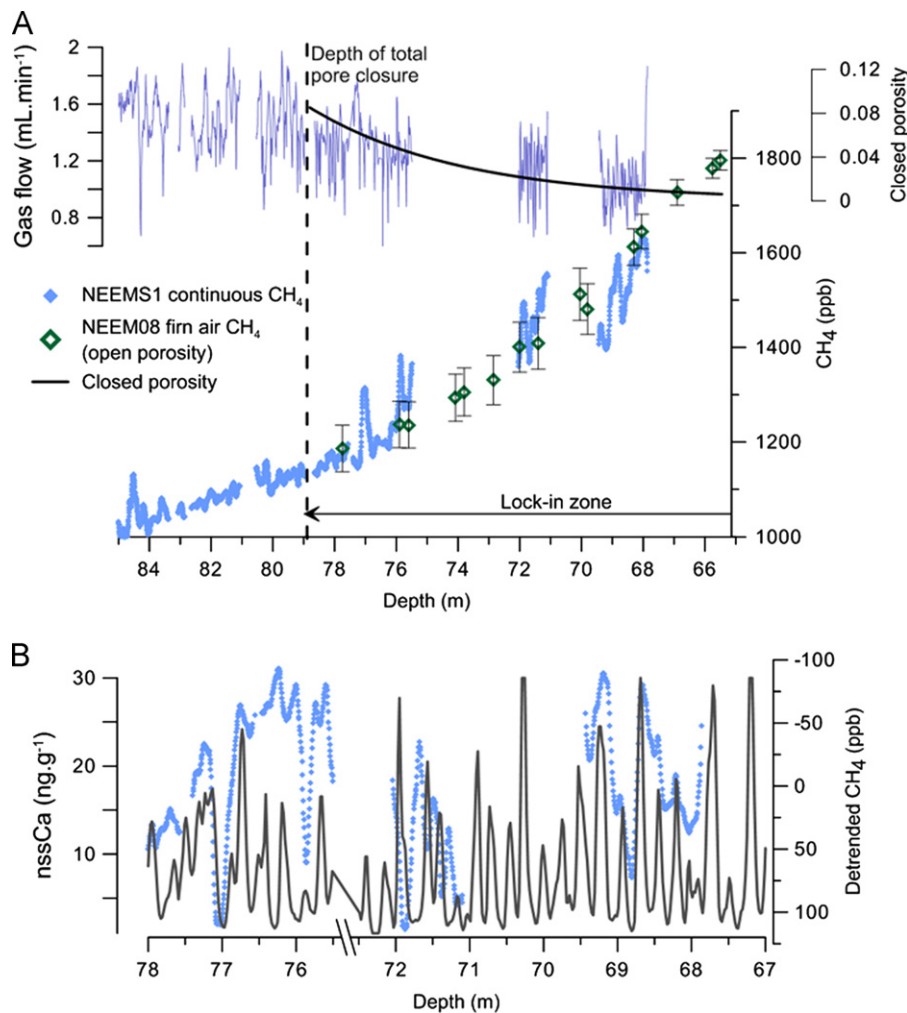
Fig. 5. (A) NEEMS1 continuous methane record between 67 and 85 m depth, including measurements of air in the closed porosity of the lock-in zone. Green diamonds are CH_4 mixing ratios of open porosity firn air sampled at the NEEM site in 2008 and black line represents the degree of closed porosity (Buizert et al., 2012). Gas flow through the laser spectrometer during analysis is also displayed (purple). (B) Detrended (linear function removed) NEEMS1 continuous methane data from the lock-in zone (note: y-axis flipped) plotted with nssCa concentrations, which exhibit spring maxima. (For interpretation of the references to colour in this figure legend, the reader is referred to the web version of this article.)

measurements of CH_4, $\delta^{13}CH_4$ and $\delta^{18}O_2$ in the basal ice of the GRIP ice core showed clear in-situ biological production of excess methane, probably in an environment corresponding to the early snow-drift accumulation before the Greenland ice sheet buildup (Souchez et al., 2006). Many viable microorganisms from GISP2 basal ice were isolated by Miteva et al. (2004) that likely originated from the basal sediment rather than aeolian input. A complete knowledge of all chemical species present in the ice, as well as information regarding the microorganisms present, is required to reach any firm conclusions about the exact pathway(s) of, or the microorganisms responsible for, the biological in-situ methane production captured in the NEEMS1 record.

Methane records retrieved from low-impurity, non-accreted ice sections of polar ice cores have, until now, displayed no signs of contamination from in-situ production and shown excellent integrity as paleoclimate archives. The close correspondence of polar methane records obtained from different ice cores, and in different hemispheres, gives confidence to the integrity of past atmospheric reconstructions (Baumgartner et al., 2012; Blunier and Brook, 2001). This is the first study to link measurements of methane and chemical impurities in polar, glacial ice (not basal or accreted ice) and to consider evidence for in-situ production in thin and infrequent layers. This is only achievable due to the high spatial resolution and precision of the continuous gas and chemistry measurements.

3.3. Continuous measurements in the firn–ice transition

The laser-based analysis system continued to analyse gas as melting proceeded up the core beyond the close-off depth at 78 m and into the lock-in zone, where the core transitions from ice to firn, and both open and closed porosity are present (Fig. 5A). Analysis ceased at 67 m with methane concentrations in the 1600 ppb range, ca. 250 ppb below ambient levels, and corresponding to trapped air dating from 1980 AD in Greenland (Kai et al., 2011). A working hypothesis is that our continuous system principally sampled air from closed porosity. As is usual when melting firn cores, some of the melted ice sample "wicked" up the core i.e., it was drawn up through the inter-connected open porosity by capillary forces (Röthlisberger et al., 2000), thereby limiting ambient air entry via the open porosity. A gradual decrease in gas flow from 1.8 mL min^{-1} below the lock-in zone to 1.0 mL min^{-1} at 67 m depth is consistent with the decrease in closed porosity with upward progression though the firn column (Fig. 5A).

We compare our results to measurements conducted on firn air, which was sampled at NEEM in 2008 by pumping from the open porosity at successive depths in a borehole (Buizert et al., 2012) (Fig. 5A). The gradient of methane increase in the NEEMS1 record is similar to that of the NEEM08 firn air measurements,

which provides confidence in our record. Many of the continuous measurements exhibit lower methane concentrations than the NEEM08 firn air. This observation is consistent with our hypothesis that the continuous method primarily sampled the closed porosity. Air in the closed porosity must be older than that in the open porosity and will therefore have a lower methane concentration as a result of the anthropogenically-induced trend of increasing methane levels in the atmosphere. However, there are several methane peaks up to 145 ppb in magnitude, which exceed the NEEM08 firn air measurements, super-imposed on the trend of gradual methane concentration increase (e.g., at 77 and 75.5 m, Fig. 5A). These are not located at depths where breaks in the ice core were recorded and do not show characteristics of in-situ production (Section 3.2.3). We note that the true signal amplitude of these spikes could be 60% larger than indicated by continuous measurements, i.e. up to 230 ppb, as a result of smoothing by the system (see Fig. 3). When plotted with an annual indicator such as nssCa, it becomes clear that the methane concentration of the air analysed varies on a quasi-annual scale (Fig. 5B). This hints that the methane variability is associated with the difference in bubble close-off time between seasonal firn layers of contrasting density (Etheridge et al., 1992; Martinerie et al., 1994). Etheridge et al. (1992) observed that low density, summer firn layers at Law Dome recorded higher methane concentrations than layers from other seasons because delayed bubble close-off in low density layers sampled younger air enriched in methane. No high resolution density data are available for this section of NEEMS1 but it has recently been proposed that increased high impurity levels promote firn densification (Hörhold et al., 2012). The coincidence of methane concentration minima with nssCa concentration maxima (Fig. 5B, note: methane axis has been flipped) therefore suggests that the impurity-rich, presumably dense layers have a greater proportion of closed porosity containing relatively old air with a lower methane concentration.

Although the NEEMS1 data from the firn–ice transition exhibit annual scale variability, the methane spikes of up to 230 ppb (unsmoothed signal) recorded in the low nssCa layers are significantly higher than firn air concentrations and are therefore unlikely to be a true reflection of the open porosity or summer layer concentration within the firn. These high magnitude spikes likely reflect some influence of ambient air, which either entered the inter-connected open porosity of the ice core during melting on the melterhead or was occluded in the closed porosity during storage after core retrieval (Aydin et al., 2010).

3.4. Quasi-annual methane oscillations in the ice

Quasi-annual scale oscillations in methane concentration are also resolved in the NEEMS1 record between 159 and 162 m depth (Fig. 6). A pervasive signal of ca. 20 cm wavelength 5–10 ppb methane oscillations is super-imposed on the trend of decreasing atmospheric concentration associated with the falling limb of the prominent methane concentration peak centred at ca. 1550 AD (Fig. 2). The variability of this section of the record was so striking that replicate cores (B Cut) were analysed using the continuous-laser method. The results clearly show that the quasi-annual scale features are reproducible (Fig. 6). The existence of this high frequency signal in the ice core is further confirmed by discrete analyses performed at 3 cm resolution on samples from 160.1–161.18 m (Fig. 6). Once again, the discrete analyses show that the continuous system causes significant signal attenuation; amplitudes recorded by the continuous method are roughly half those measured by the discrete method.

As the quasi-annual oscillations in methane are resolved across a time interval (1546–1560 AD) of decreasing atmospheric
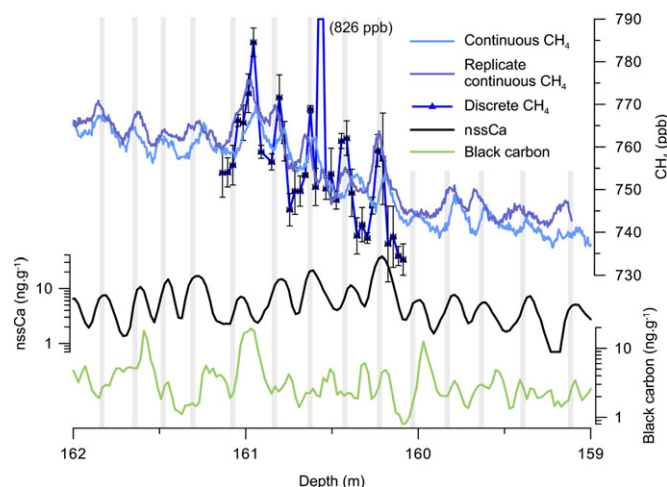
Fig. 6. Quasi-annual frequency, low amplitude oscillations in methane concentration resolved and replicated (B cut core) by the continuous-laser technique. Also plotted are nssCa and black carbon records. Grey bars indicate depths of January 1st for 1364–1378 AD (ice age). Methane variability is confirmed by gas chromatography measurements on discrete samples at 3 cm depth resolution. Uncertainty bars are 2σ. Offset in depth between the CH$_4$ datasets is within the stated ± 3 cm uncertainty (1σ).

methane concentrations (-2 ppb yr^{-1}), it can be hypothesised that they result from staggering in the timing of air bubble trapping between layers of contrasting density, as discussed in Section 3.3. Critically, we observe that the methane oscillations and nssCa annual peaks occur in phase (Fig. 6), opposite phasing to that seen across the firn–ice transition (Fig. 5B). This is consistent with a decreasing trend in atmospheric concentration, as opposed to an increasing trend, during bubble close-off. If the outlying data point in the discrete dataset at 160.57 m depth is ignored (Fig. 6), the mean methane concentration difference between peak and trough values is 24 ppb. Given the underlying trend in atmospheric methane of -2 ppb yr^{-1} this would indicate a 12 yr offset in bubble close-off time between adjacent layers.

Our hypothesis that staggered bubble close-off is responsible for the quasi-annual signals in the NEEMS1 ice core would be strengthened if no high frequency variability was recorded for time intervals when the atmospheric methane level was stable but this is not the case. Whilst no other section of the ice core exhibits the pervasive quasi-annual features shown on Fig. 6, variability in the methane signal at the sub-metre scale (sub-decadal temporal scale) is not unique to that depth range. Differentiating true signal from noise is challenging without replicate data. Available replicate data for other depth intervals suggest that some sub-metre scale features are reproducible (Fig. S5). An alternative hypothesis could be that in-situ biological production is responsible for all the high frequency variability in NEEMS1 record. However, we note that whereas elevated black carbon levels are clearly linked to the abrupt, high amplitude in-situ methane spikes identified in Table 2, the high frequency, low amplitude methane oscillations show little correspondence with the phasing or amplitudes of black carbon peaks (Figs. 6 and S5).

We conclude that a combination of staggered bubble close-off, biological in-situ production and possibly other unidentified mechanisms may simultaneously create high frequency (sub-metre scale) artifacts in the ice core methane signal. A good method to delineate between the influence of physical and biological mechanisms would be measurement of δ^{13}CH$_4$ across the methane peaks.

4. Conclusions

Continuous analysis of the methane concentration of ancient air trapped in bubbles within the NEEMS1 ice core produced three key findings:

- The multi-decadal variability in atmospheric methane over the last 1800 yr is faithfully replicated by our continuous dataset and the NEEMS1 record is testament to the detailed resolution (5 cm), fast data acquisition time (30 m day^{-1}) and excellent long-term reproducibility (2.6% 2RSD) achievable using the continuous measurement technique.
- Abrupt (20–100 cm depth interval), high amplitude (35–80 ppb excess) methane spikes detected by the continuous system are replicated by discrete measurements. Comparison of these methane spikes and co-registered glaciochemical data highlights that excess methane levels are associated with elevated concentrations of black carbon, ammonium and nitrate. It is suggested that the abrupt, high amplitude methane spikes may result from very localised biological in-situ production in polar, glacial ice. This does not affect the long-term trends of the methane signals observed in the NEEM ice cores. Moreover, this study highlights that continuous trace gas measurements facilitate the detection of ice layers rich in microbial activity, which is useful for both objective exclusion of contaminated data points and the investigation of in-situ trace gas production.
- Measurements of air from the firn–ice transition suggest that quasi-annual scale methane oscillations likely created by staggering of bubble close-off times in adjacent layers, resulting from density contrasts that are possibly linked to impurity content, can be resolved. Further investigation is required to understand to what extent the observed signals reflect real variability in composition of the firn air, as opposed to ambient air contamination artifacts. Quasi-annual scale oscillations in methane concentration resolved in a deeper section (1546–1560 AD), and reproduced by the continuous technique and gas chromatography-based discrete measurements, suggest that high frequency artifacts of staggered bubble close-off are preserved in the ice. However, other portions of the record display resolvable and reproducible high frequency (sub-metre/sub-decadal scale) signal that it is difficult to attribute to the bubble trapping process and which may be related to in-situ production or an unknown mechanism.

Appendix A. Supporting information

Supplementary data associated with this article can be found in the online version at http://dx.doi.org/10.1016/j.epsl.2013.02.034.

References

Allan, D., 1966. Statistics of atomic frequency standards. Proc. IEEE 54, 221–230.

Anklin, M., Schwander, J., Stauffer, B., Tschumi, J., Fuchs, A., 1997. CO_2 record between 40 and 8 kyr B.P. from the Greenland Ice Core Project ice core. J. Geophys. Res. 102, 26539–26545.

Aydin, M., Montzka, S.A., Battle, M.O., Williams, M.B., De Bruyn, W.J., Butler, J.H., Verhulst, K.R., Tatum, C., Gun, B.K., Plotkin, D.A., Hall, B.D., Saltzman, E.S., 2010. Post-coring entrapment of modern air in some shallow ice cores collected near the firn-ice transition: evidence from CFC-12 measurements in Antarctic firn air and ice cores. Atmos. Chem. Phys. 10, 5135–5144.

Barnes, P.R.F., Wolff, E.W., 2004. Distribution of soluble impurities in cold glacial ice. J. Glaciol. 50, 311–324.

Barnola, J.M., Anklin, M., Porcheron, J., Raynaud, D., Schwander, J., Stauffer, B., 1995. CO_2 evolution during the last millennium as recorded by Antarctic and Greenland ice. Tellus B 47, 264–272.

Baumgartner, M., Schilt, A., Eicher, O., Schmitt, J., Schwander, J., Spahni, R., Fischer, H., Stocker, T.F., 2012. High-resolution interpolar difference of atmospheric methane around the Last Glacial Maximum. Biogeosciences 9, 3961–3977.

Bigler, M., Svensson, A., Kettner, E., Vallelonga, P., Nielsen, M.E., Steffensen, J.P., 2011. Optimization of high-resolution continuous flow analysis for transient climate signals in ice cores. Environ. Sci. Technol. 45, 4483–4489.

Blunier, T., Brook, E.J., 2001. Timing of millennial-scale climate change in Antarctica and Greenland during the last glacial period. Science 291, 109–111.

Blunier, T., Chappellaz, J., Schwander, J., Stauffer, B., Raynaud, D., 1995. Variations in atmospheric methane concentration during the Holocene epoch. Nature 374, 46–49.

Blunier, T., Spahni, R., Barnola, J.-M., Chappellaz, J., Loulergue, L., Schwander, J., 2007. Synchronization of ice core records via atmospheric gases. Clim. Past 3, 325–330.

Brook, E.J., Harder, S., Severinghaus, J., Steig, E.J., Sucher, C.M., 2000. On the origin and timing of rapid changes in atmospheric methane during the Last Glacial Period. Global Biogeochem. Cycles 14, 559–572.

Buizert, C., Martinerie, P., Petrenko, V.V., Severinghaus, J.P., Trudinger, C.M., Witrant, E., Rosen, J.L., Orsi, A.J., Rubino, M., Etheridge, D.M., Steele, L.P., Hogan, C., Laube, J.C., Sturges, W.T., Levchenko, V.A., Smith, A.M., Levin, I., Conway, T.J., Dlugokencky, E.J., Lang, P.M., Kawamura, K., Jenk, T.M., White, J.W.C., Sowers, T., Schwander, J., Blunier, T., 2012. Gas transport in firn: multiple-tracer characterisation and model intercomparison for NEEM, Northern Greenland. Atmos. Chem. Phys. 12, 4259–4277.

Christner, B.C., Mosley-Thompson, E., Thompson, L.G., Zagorodnov, V., Sandman, K., Reeve, J.N., 2000. Recovery and identification of viable bacteria immured in glacial ice. Icarus 144, 479–485.

Dlugokencky, E.J., Myers, R.C., Lang, P.M., Masarie, K.A., Crotwell, A.M., Thoning, K.W., Hall, B.D., Elkins, J.W., Steele, L.P., 2005. Conversion of NOAA atmospheric dry air CH_4 mole fractions to a gravimetrically prepared standard scale. J. Geophys. Res. 110, http://dx.doi.org/10.1029/2005JD006035.

Etheridge, D., Pearman, G.I., Fraser, P.J., 1992. Changes in tropospheric methane between 1841 and 1978 from a high accumulation-rate Antarctic ice core. Tellus B 44, 282–294.

Etheridge, D.M., Steele, L.P., Francey, R.J., Langenfelds, R.L., 1998. Atmospheric methane between 1000 AD and present: evidence of anthropogenic emissions and climatic variability. J. Geophys. Res. 103, 15979–15993.

Faïn, X., Rhodes, R.H., Stowasser, C. Chappellaz, J., Blunier, T., McConnell, J.R., Brook, E.J., Legrand, M., Debois, T., Romanini, D. High resolution measurements of carbon monoxide along the top 400 m of the NEEM core: evidence for in-situ production, in preparation.

Flückiger, J., Monnin, E., Stauffer, B., Schwander, J., Stocker, T.F., Chappellaz, J., Raynaud, D., Barnola, J.-M., 2002. High-resolution Holocene N_2O ice core record and its relationship with CH_4 and CO_2. Global Biogeochem. Cycles 16, 1010.

Gkinis, V., Popp, T.J., Blunier, T., Bigler, M., Schüpbach, S., Kettner, E., Johnsen, S.J., 2011. Water isotopic ratios from a continuously melted ice core sample. Atmos. Meas. Tech. 4, 2531–2542.

Grachev, A.M., Brook, E.J., Severinghaus, J.P., 2007. Abrupt changes in atmospheric methane at the MIS 5b–5a transition. Geophys. Res. Lett. 34, http://dx.doi.org/10.1029/2007GL029799.

Grachev, A.M., Brook, E.J., Severinghaus, J.P., Pisias, N.G., 2009. Relative timing and variability of atmospheric methane and GISP2 oxygen isotopes between 68 and 86 ka. Global Biogeochem. Cycles 23, http://dx.doi.org/10.1029/2008GB003330.

Hörhold, M.W., Laepple, T., Freitag, J., Bigler, M., Fischer, H., Kipfstuhl, S., 2012. On the impact of impurities on the densification of polar firn. Earth Planet. Sci. Lett. 325–326, 93–99.

Kai, F.M., Tyler, S.C., Randerson, J.T., Blake, D.R., 2011. Reduced methane growth rate explained by decreased North Hemisphere microbial sources. Nature 476, 194–197.

Kaufmann, P.R., Federer, U., Hutterli, M.A., Bigler, M., Schüpbach, S., Ruth, U., Schmitt, J., Stocker, T.F., 2008. An improved continuous flow analysis system for high-resolution field measurements on ice cores. Environ. Sci. Technol. 42, 8044–8050.

Lelieveld, J.O.S., Crutzen, P.J., Dentener, F.J., 1998. Changing concentration, lifetime and climate forcing of atmospheric methane. Tellus B 50, 128–150.

Loulergue, L., Schilt, A., Spahni, R., Masson-Delmotte, V., Blunier, T., Lemieux, B., Barnola, J.-M., Raynaud, D., Stocker, T.F., Chappellaz, J., 2008. Orbital and millennial-scale features of atmospheric CH_4 over the past 800,000 years. Nature 453, 383–386.

MacFarling Meure, C., Etheridge, D., Trudinger, C., Steele, P., Langenfelds, R., van Ommen, T., Smith, A., Elkins, J., 2006. Law Dome CO_2, CH_4 and N_2O ice core records extended to 2000 years BP. Geophys. Res. Lett. 33, http://dx.doi.org/10.1029/2006GL026152.

Martinerie, P., Lipenkov, V.Y., Raynaud, D., Chappellaz, J., Barkov, N.I., Lorius, C., 1994. Air content paleo record in the Vostok ice core (Antarctica): A mixed record of climatic and glaciological parameters. J. Geophys. Res. 99, 10565–10576.

McConnell, J.R., Edwards, R., 2008. Coal burning leaves toxic heavy metal legacy in the Arctic. Proc. Natl. Acad. Sci., http://dx.doi.org/10.1073/pnas.0803564105.

McConnell, J.R., Edwards, R., Kok, G.L., Flanner, M.G., Zender, C.S., Saltzman, E.S., Banta, J.R., Pasteris, D.R., Carter, M.M., Kahl, J.D.W., 2007. 20th-century industrial black carbon emissions altered Arctic climate forcing. Science 317, 1381–1384.

McConnell, J.R., Lamorey, G.W., Lambert, S.W., Taylor, K.C., 2002. Continuous ice-core chemical analyses using inductively coupled plasma mass spectrometry. Environ. Sci. Technol. 36, 7–11.

Menviel, L., Timmermann, A., Timm, O.E., Mouchet, A., 2011. Deconstructing the Last Glacial termination: the role of millennial and orbital-scale forcings. Quat. Sci. Rev. 30, 1155–1172.

Mitchell, L.E., Brook, E.J., Lee, J.E., Buizert, C., Sowers, T. New constraints on the Late Holocene anthropogenic contribution to the methane budget, in preparation.

Mitchell, L.E., Brook, E.J., Sowers, T., McConnell, J.R., Taylor, K., 2011. Multidecadal variability of atmospheric methane, 1000–1800 C.E. J. Geophys. Res. 116, http://dx.doi.org/10.1029/2010JG001441.

Miteva, V.I., Sheridan, P.P., Brenchley, J.E., 2004. Phylogenetic and physiological diversity of microorganisms isolated from a deep Greenland glacier ice core. Appl. Environ. Microbiol. 70, 202–213.

Morville, J., Kassi, S., Chenevier, M., Romanini, D., 2005. Fast, low-noise, mode-by-mode, cavity-enhanced absorption spectroscopy by diode-laser self-locking. Appl. Phys. B Lasers Opt. 80, 1027–1038.

NEEM community members, 2013. Eemian interglacial reconstructed from a Greenland folded ice core. Nature 493, 489–494.

NIST, 2011. National Institute of Standards and Technology Standard Reference Database, ⟨http://webbook.nist.gov/chemistry/form-ser.html⟩.

Price, P.B., 2000. A habitat for psychrophiles in deep Antarctic ice. Proc. Natl. Acad. Sci. 97, 1247–1251.

Price, P.B., 2007. Microbial life in glacial ice and implications for a cold origin of life. FEMS Microbiol. Ecol. 59, 217–231.

Rohde, R.A., Price, P.B., Bay, R.C., Bramall, N.E., 2008. In situ microbial metabolism as a cause of gas anomalies in ice. Proc. Natl. Acad. Sci. 105, 8667–8672.

Romanini, D., Chenevier, M., Kassi, S., Schmidt, M., Valant, C., Ramonet, M., Lopez, J., Jost, H.J., 2006. Optical-feedback cavity-enhanced absorption: a compact spectrometer for real-time measurement of atmospheric methane. Appl. Phys. B Lasers Opt. 83, 659–667.

Röthlisberger, R., Bigler, M., Hutterli, M., Sommer, S., Stauffer, B., Junghans, H.G., Wagenbach, D., 2000. Technique for continuous high-resolution analysis of trace substance in firn and ice cores. Environ. Sci. Technol. 34, 338–343.

Schüpbach, S., Federer, U., Kaufmann, P.R., Hutterli, M.A., Buiron, D., Blunier, T., Fischer, H., Stocker, T.F., 2009. A new method for high-resolution methane measurements on polar ice cores using continuous flow analysis. Environ. Sci. Technol. 43, 5371–5376.

Schwander, J., Sowers, T., Barnola, J.M., Blunier, T., Fuchs, A., Malaizé, B., 1997. Age scale of the air in the summit ice: implication for glacial–interglacial temperature change. J. Geophys. Res. 102, 19483–19493.

Sigl, M., McConnell, J.R., Layman, L., Maselli, O., McGwire, K., Pasteris, D., Jensen, D.D., Steffensen, J.P., Edwards, R., Mulvaney, R. A new bipolar ice core record of volcanism from WAIS Divide and NEEM and implications for climate forcing of the last 2000 years. J. Geophys. Res. http://dx.doi.org/10.1029/2012JD018603, in press.

Singarayer, J.S., Valdes, P.J., Friedlingstein, P., Nelson, S., Beerling, D.J., 2011. Late Holocene methane rise caused by orbitally controlled increase in tropical sources. Nature 470, 82–87.

Souchez, R., Jouzel, J., Landais, A., Chappellaz, J., Lorrain, R., Tison, J.-L., 2006. Gas isotopes in ice reveal a vegetated central Greenland during ice sheet invasion. Geophys. Res. Lett. 33, http://dx.doi.org/10.1029/2006GL028424.

Spahni, R., Schwander, J., Flückiger, J., Stauffer, B., Chappellaz, J., Raynaud, D., 2003. The attenuation of fast atmospheric CH_4 variations recorded in polar ice cores. Geophys. Res. Lett. 30, 1571, http://dx.doi.org/10.1029/2003GL017093.

Stowasser, C., Buizert, C., Gkinis, V., Chappellaz, J., Schüpbach, S., Bigler, M., Faïn, X., Sperlich, P., Baumgartner, M., Schilt, A., Blunier, T., 2012. Continuous measurements of methane mixing ratios from ice cores. Atmos. Meas. Tech. 5, 999–1013.

Tschumi, J., Stauffer, B., 2000. Reconstructing past atmospheric CO_2 concentration based on ice-core analyses: open questions due to in situ production of CO_2 in the ice. J. Glaciol. 46, 45–53.

Tung, H.C., Bramall, N.E., Price, P.B., 2005. Microbial origin of excess methane in glacial ice and implications for life on Mars. Proc. Natl. Acad. Sci. 102, 18292–18296.